QUANTIFYING UNCERTAINTIES IN MEAN ABSORPTION COEFFICIENTS FOR A WALL-STABILIZED ELECTRIC ARC

R. Fuchs*, H. Nordborg

Institute for Energy Technology, HSR University of Applied Sciences Rapperswil, Oberseestrasse 10, 8640 Rapperswil, Switzerland

* roman.fuchs@hsr.ch

Abstract. The quality of arc simulations depends significantly on radiation modeling. Uncertainties due to physical parameters and modeling errors should be systematically quantified. We solve the energy balance equation for a wall-stabilized arc using the P1 model, i.e. without a prescribed temperature profile. We derive the linearized equation and assess the arc voltage sensitivity. This method allows us to optimize the definition of mean absorption coefficients consistently and at low computational costs.

Keywords: sensitivity, mean absorption coefficient, P1 model, optimization, arc simulation.

1. Introduction

Electric arcs and their numerical modeling in industrial devices lead to a diverse set of questions raising many separate research topics. One of them is radiation, since electrical arcs dissipate enormous amounts of thermal energy leading to elevated temperature levels. Therefore, radiation is almost always an important energy transfer mode in electrical arcs.

The basic relations of radiation are given by the radiative transfer equation (RTE)

$$\hat{s} \cdot \nabla I_\nu = \kappa_\nu (B_\nu - I_\nu), \qquad (1)$$

which is stated here for the simplest case of a non-scattering medium in local thermal equilibrium (LTE).[1] It describes the change of radiative intensity I_ν along direction $\hat{s}$ that is due to emission, described by the Planck function B_ν and given in equation (5) below, and absorption of the medium. Solving the RTE is computationally demanding since the radiative intensity is a function of location, direction, and frequency. The absorption coefficient κ_ν and its impact on the computational complexity of the RTE are discussed subsequently.

To meet the limited computer resources available to application engineers, the complexity of the RTE must be reduced to simpler models that account appropriately for the radiative thermal energy transport. The method of net emission coefficients (NEC) [2] is often used and has been developed to acceptable accuracy [3]. Its main advantage lies in the marginal computational costs incurred at run time of a plasma simulation, since the radiative thermal source term is tabulated in advance. However, evaluating the radiative heat flux on a nearby surface requires more sophisticated methods. One option is the P1 model, which is a first-order approximation of the RTE in spherical harmonics and frequently used in industrial arc simulations. This model leads to additional differential equations that are of the same structure as
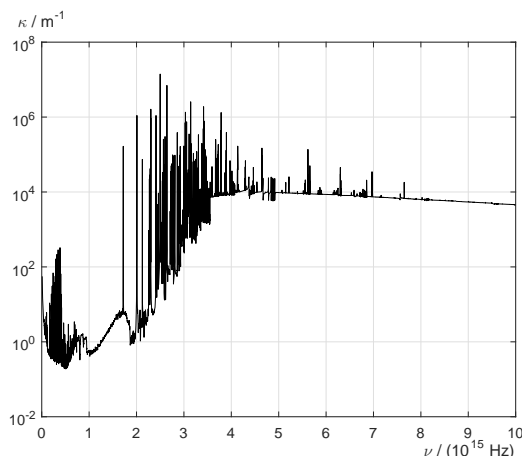

Figure 1. Absorption spectrum of air at $T = 10\,kK$. [4]

the conservation equations for mass, momentum, and energy.

We also have to consider the material data. The most important quantity in radiation modeling is the spectral absorption coefficient κ_ν, which depends on the radiation frequency ν, gas pressure, temperature, and gas composition. The complex structure of the absorption spectrum (see figure 1) is due to the atomic structure of the gas (see, e.g., [1]). It does not allow for a naive usage of this data, since an appropriate resolution of the frequency domain would lead to excessive computational costs. Despite the large variations in the value of the absorption coefficient, the frequency domain is split into a small number of intervals or bands and mean absorption coefficients (MAC) are computed for each of them. Since each frequency band acts as a gray body, this approach is termed as the multi-banded gray P1 model.

The main problem of the averaging step is how the absorption lines shall be treated that span over multiple orders of magnitudes. Classically, the Planck and Rosseland average are considered which are weighted

averages of κ_ν and κ_ν^{-1}, respectively. The former is dominated by the peak values of the absorption lines while the latter almost ignores them. It is clear that the MAC depend on the definition of the frequency band boundaries that are often chosen heuristically.

The raw data itself comes with uncertainties that affect the MAC values and propagate to the final results. Their sensitivities can be quantified by running simulations repeatedly with slightly edited input data, but comes with major computational costs. For small changes in the MAC, however, we will show that the same information can be obtained much quicker by deriving the linearized equations and solving for the first-order effects on the temperature profile and the quantities depending on it. Such modeling errors are often studied using a fixed temperature profile. From a physical point of view it makes more sense to solve the energy conservation equation, since any change in the radiation model results in an updated temperature field and, consequently, other quantities such as arc voltage.

In this paper, we quantify modeling errors in the mean absorption coefficient that are due to the averaging procedure or inherent to the raw data itself. We iteratively solve the energy balance equation for a wall-stabilized arc to ensure energy conservation. Ultimately, we present the linearized equations as a validated and computationally efficient methodology to determine first-order effects on the arc voltage.

2. Model

2.1. Energy conservation equation

We consider a wall-stabilized arc, i.e. a cylindrical plasma column of radius R, large aspect ratio, and a fixed wall temperature. Moreover, we assume that the plasma is in local thermal equilibrium (LTE) so that the pressure p and electric field E are constant across the plasma column. Further, convective heat transfer is considered weak enough to be negligible. This results in a temperature profile $T(r)$ that only depends on the arc radius r. In this case, the energy conservation equation consists of heat conduction, Ohmic heating, and a radiative heat sink U,

$$\mathrm{div}(-\lambda \, \mathrm{grad}(T)) = \sigma E^2 + U; \qquad (2)$$

here, $\lambda(T)$ and $\sigma(T)$ denote the thermal and electrical conductivities. The electric field is given as the ratio of electric current I to the plasma conductivity $S[T]$, which is a functional of the temperature profile:

$$E = \frac{I}{S[T]}, \quad S[T] = \int_0^R \sigma(T(r)) r \, \mathrm{d}r. \qquad (3)$$

In this model, we consider the current as a constant.

The radiative heat sink U is given by the divergence of the total radiative heat flux. We use the multi-banded gray P1 model to account for radiative heat transfer. Hence, we split the spectral domain into a finite number of intervals $D_i = [\nu_{i-1}, \nu_i]$. The mean

absorption coefficients $\kappa_i = \langle \kappa \rangle_i$ are obtained using the Planck and Rosseland average

$$\langle \kappa \rangle_i^{Pl} = \frac{\int_{D_i} B_\nu \kappa_\nu \, \mathrm{d}\nu}{\int_{D_i} B_\nu \, \mathrm{d}\nu}, \quad \langle \kappa \rangle_i^{Ro} = \frac{\int_{D_i} B_\nu' \, \mathrm{d}\nu}{\int_{D_i} B_\nu' \kappa_\nu^{-1} \, \mathrm{d}\nu}, \quad (4)$$

respectively. Therein, $B_\nu(T)$ denotes the Planck function

$$B_\nu(T) = \frac{2h}{c^2} \frac{\nu^3}{\exp(\frac{h\nu}{k_B T}) - 1}, \qquad (5)$$

B_ν' is its derivative with respect to temperature, c denotes the speed of light in vacuum, and h, k_B are the Planck and Boltzmann constants, respectively. The P1 model approximation results in an expression relating the radiative heat flux $\vec{F}_\nu$ and the irradiation function G_ν by:

$$\vec{F}_\nu = \frac{-1}{3\kappa_\nu} \, \mathrm{grad}(G_\nu). \qquad (6)$$

This also holds for band-averaged quantities, so that G_i is obtained as the solution of the linear problem

$$\mathcal{L}_i(G_i) := \mathrm{div}\left(\frac{-1}{3\kappa_i} \, \mathrm{grad}(G_i)\right) + \kappa_i(G_i) = \kappa_i 4\pi B_i(T) \qquad (7)$$

with $B_i(T)$ denoting the band-integrated Planck function. The radiative heat sink is then given by

$$U = (-1) \sum_i \kappa_i (4\pi B_i(T) - G_i), \qquad (8)$$

which follows from the RTE (1) by integration over the solid angle.

2.2. Linearized equation

Equations (2) and (8) show that any change in the absorption coefficient results in changes to the temperature profile. For small variations, we can derive the linearized energy conservation equation with respect to increments in the MAC ($\delta \kappa_i$) and temperature (δT). This first-order expansion provides a relation which we write as

$$C_{th}(\delta T) - M_I(\delta T) = \delta U, \qquad (9)$$

with $\delta U = \delta U(\delta \kappa_i, \delta T)$ summarizing the linear effects in the radiation model. The details are derived in the remainder of this section.

The linearized heat conduction is given by

$$\begin{aligned} C_{th}(\delta T) = {} & \mathrm{div}\left(-\lambda(T) \, \mathrm{grad}(\delta T)\right) \\ & - \mathrm{div}\left(\lambda'(T) \, \mathrm{grad}(T) \delta T\right), \end{aligned} \qquad (10)$$

with $\lambda'(T) = \frac{\mathrm{d}}{\mathrm{d}T}\lambda(T)$. The linearized Ohmic heating at constant current results in

$$M_I(\delta T) = \left(\sigma'(T) - 2\frac{\sigma(T)}{S[T]}\frac{\delta S[T]}{\delta T(r)}\right)\frac{I^2}{S[T]^2}\delta T \quad (11)$$

where $\frac{\delta S[T]}{\delta T(r)}$ represents the functional derivative of the conductivity, $\sigma'(T) = \frac{d}{dT}\sigma(T)$, and the radiative heat sink increment is expanded to

$$\begin{aligned}\delta U = (-1)\sum_i (4\pi B_i(T) - G_i)\delta\kappa_i \\ +\kappa_i(4\pi B_i'(T)\delta T - \delta G_i).\end{aligned} \quad (12)$$

The linear increment in the irradiation function δG_i is obtained as the solution of

$$\delta G_i = \mathcal{L}_i^{-1}(M_{\kappa,i}\delta\kappa_i + M_{th,i}\delta T) \quad (13)$$

with

$$\begin{aligned}M_{\kappa,i}(\delta\kappa_i) = \text{div}\left(\frac{-1}{3\kappa_i^2}\text{grad}(G_i)\delta\kappa_i\right) \\ +(4\pi B_i(T) - G_i)\delta\kappa_i,\end{aligned} \quad (14)$$

$$M_{th,i}(\delta T) = \kappa_i 4\pi B_i'(T)\delta T. \quad (15)$$

In summary, the terms can be rearranged so that the increment in the temperature profile is given as a linear function of those in the MACs,

$$\delta T = Z^{-1}\sum_i Y_i\delta\kappa_i, \quad (16)$$

with Z and Y being linear operators given by

$$Z := C_{th} - M_I + \sum_i \kappa_i 4\pi B_i'(T) - \kappa_i\mathcal{L}_i^{-1}M_{th,i}, \quad (17)$$

$$Y_i := \kappa_i\mathcal{L}_i^{-1}M_{th,i} - (4\pi B_i(T) - G_i). \quad (18)$$

Finally, we find an expression for the linear increment in the electric field with respect to a temperature increment:

$$\delta E = (-1)\frac{I}{S^2[T]}\frac{\delta S[T]}{\delta T(r)}\delta T. \quad (19)$$

2.3. Simulation conditions

We use a domain radius of $R = 5\,\text{mm}$ discretized with 200 cells and cell-centered quantities. The wall temperature is fixed at $300\,\text{K}$. The energy conservation equation (2) is iteratively solved using a relaxation update with a constant current of $I = 50\,\text{A}$ until the maximal temperature update is smaller than $1\,\text{K}$.

The radiation frequency bands are defined as N uniformly spaced intervals $D_i = [\nu_{i-1}, \nu_i]$, $i = 1, \ldots, N$, with $\nu_0 = 10^{10}\,\text{Hz}$ and $\nu_N = 6 \times 10^{15}\,\text{Hz}$. An additional frequency band is defined $D_{N+1} = [\nu_N, 10^{16}\,\text{Hz}]$. Material data and spectral absorption coefficients are taken for air at $p = 10\,\text{bar}$.[4]
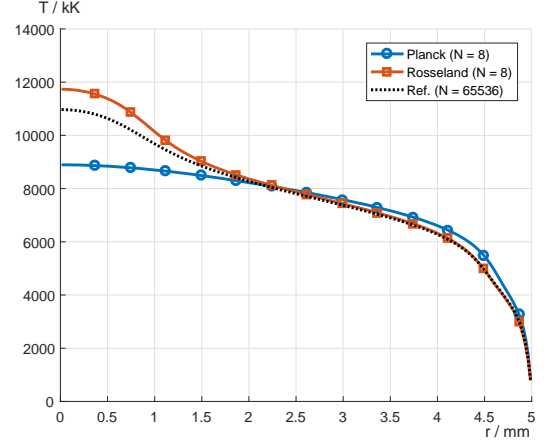
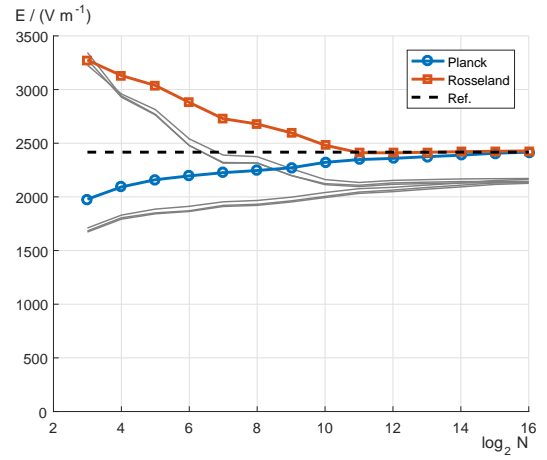*Figure 2. Temperature profiles at* $50\,\text{A}$ *total current.*

Figure 3. Electric field at $50\,\text{A}$ *total current as a function of spectral resolution. The reference value is taken for the finest spectral resolution. Gray lines:* 100, 150, *and* $200\,\text{A}$.

3. Results and Discussion

Figure 2 shows temperature profiles of the wall-stabilized arc obtained with Planck and Rosseland average using 8 bands. We also plot the reference solution with $N = 65536$ bands, which shows an arc center temperature of $10970\,\text{K}$ and a noticeable core region with a higher temperature gradient than in the outer parts. Near the wall, the temperature drops quickly to the prescribed wall temperature. In comparison to this, the Rosseland average leads to a more pronounced core region with a higher arc center temperature but qualitatively similar temperature profile. In contrast, the Planck average shows a diffusive temperature profile with an arc center temperature much lower than the reference solution, and a sightly increased temperature in the outer parts. These differences disappear gradually with finer spectral resolutions and the temperature profiles converge to the reference solution.

This data is explained by the properties of the averaging methods. Since the Planck average is dominated by the peak values of the absorption lines, it resem-

bles an optically thick plasma, and the radiative heat transfer has the same effect as an increased thermal conductivity. On the other hand, the Rosseland average yields an optically thin material and radiative energy is transported to the walls.

Figure 3 shows the electric field in variation of the spectral resolution and for several arc currents. We see that, at low spectral resolutions, the Planck average yields a higher electric field than the Rosseland average. This is due to the lower temperature levels and lower electrical conductivity. We also note that the curves converge to the reference solution, with the Planck average being rather constant for spectral resolutions $N > 2^{10}$. This figure shows that accurate results are only obtained with a finely resolved absorption spectrum.

We now turn to the question, which parts of the spectrum are most significant. Figure 4 and 5 show the relative sensitivity of the electric field obtained by the linearized equation for the two averaging methods. We used an uncertainty of 1% in the MAC for each band individually. The same data is also obtained with direct computations for $N \leq 256$, i.e. editing the MAC values and running the simulation until convergence, but at much higher computational costs. The results coincide almost exactly and validate the linearized method. Only minor differences are noted for the solution using $N = 8$ bands and Rosseland average: however, they are at higher radiation frequencies where the sensitivities are orders of magnitudes lower and therefore negligible. This method has also been applied to finely resolved spectral data with drastically reduced computational effort.

The sensitivity of the electric field is limited by 1‰ for the 8-banded solution. The sensitivity curves scale with the interval length; in fact, considering the relative sensitivity of the electric field per interval length, i.e. $\Delta E/(E_{ref}\Delta\nu)$, results in a characteristic curve. We also see that a higher number of spectral bands allows to resolve the sensitivities of the absorption lines. The sensitivity curve of a finer resolved solution is bounded almost everywhere by the coarser ones. The Planck average yields notable lower sensitivities at frequencies above 2.5×10^{15} Hz and band resolutions $N \leq 256$.

4. Conclusions

We presented a simple model to study effects of band-averaged MACs on the temperature profile and the electric field of a wall-stabilized arc. The linearized method provides a systematic methodology to assess the sensitivity of the frequency bands at low computational costs, and helps to define MAC inside each band. Hence, frequency bands of low sensitivity can be identified and may be merged or grouped into coarser ones. For future work, the method is easily extended to non-uniform intervals. Preliminary tests with a renormalization length [5] are promising and are currently being investigated.
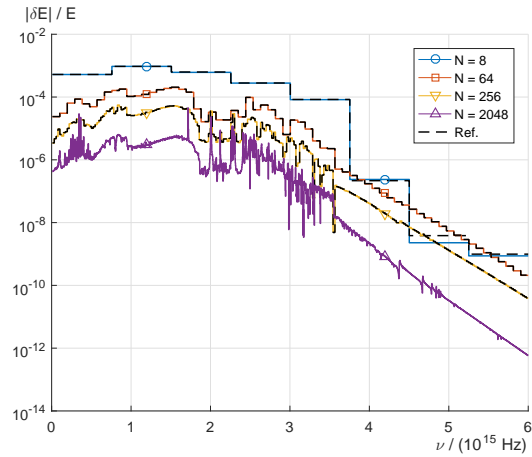
Figure 4. Relative sensitivity of the electric field at 50 A *using Rosseland average and uncertainty of 1%.*
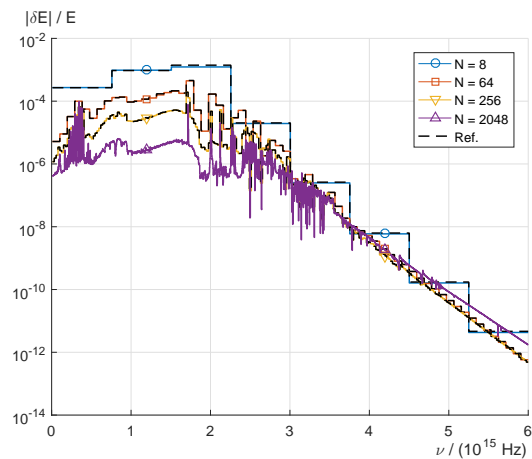

Figure 5. Relative sensitivity of the electric field at 50 A *using Planck average and uncertainty of 1%.*

References

[1] M. F. Modest. *Radiative heat transfer*. Elsevier Science, San Diego, third edition, 2013.

[2] J. J. Lowke. Predictions of arc temperature profiles using approximate emission coefficients for radiation losses. *J Quant Spect and Rad Transfer*, 14(2):111–122, 1974. `doi:10.1016/0022-4073(74)90004-1`.

[3] H. Z. Randrianandraina, Y. Cressault, and A. Gleizes. Improvements of radiative transfer calculation for SF 6 thermal plasmas. *J Phys D: Appl Phys*, 44(19):194012, 2011. `doi:10.1088/0022-3727/44/19/194012`.

[4] P. Kloc, V. Aubrecht, M. Bartlova, and O. Coufal. Radiation transfer in air and air-Cu plasmas for two temperature profiles. *J Phys D: Appl Phys*, 48(5):055208, 2015. `doi:10.1088/0022-3727/48/5/055208`.

[5] H. Nordborg and A. A. Iordanidis. Self-consistent radiation based modelling of electric arcs: I. Efficient radiation approximations. *J Phys D: Appl Phys*, 41(13):135205, 2008. `doi:10.1088/0022-3727/41/13/135205`.